

NATIONAL AIR INTELLIGENCE CENTER



**HIGH-RESOLUTION TeO_2 ACOUSTO-OPTICAL DEFLECTOR
FOR MILLIMETER-WAVE SPECTROMETER**

by

**Xu Binghuo, Zhao Guozhen, Bian Huian,
Chu Haiqun and Jin Jianhui**



Approved for public release;
Distribution unlimited.

19950407 126

DTIC QUALITY INSPECTED 5

HUMAN TRANSLATION

NAIC-ID(RS)T-0412-94

22 February 1995

MICROFICHE NR:

High-Resolution TeO₂ Acousto-Optical Deflector for Millimeter-Wave Spectrometer

By: Xu Binghuo, Zhao Guozhen, Bian Huian, Chu Haiqun and Jin Jianhui

English pages: 10

Source: YINGYONG JIGUANG, VOL 8, NR 6, DECEMBER 1988

Country of origin: CHINA
 This document is a Human translation.
 Translated by: Leo Kanner Ass.
 Merged by: Ruth Peterson
 Requester: NAIC/TATA/J. FINLEY
 Approved for public release; Distribution unlimited.

Accession For	
NTIS CRA&I	<input checked="" type="checkbox"/>
DTIC TAB	<input type="checkbox"/>
Unannounced	<input type="checkbox"/>
Justification	
By	
Distribution /	
Availability Codes	
Dist	Avail and/or Special
A-1	

THIS TRANSLATION IS A RENDITION OF THE ORIGINAL FOREIGN TEXT WITHOUT ANY ANALYTICAL OR EDITORIAL COMMENT STATEMENTS OR THEORIES ADVOCATED OR IMPLIED ARE THOSE OF THE SOURCE AND DO NOT NECESSARILY REFLECT THE POSITION OR OPINION OF THE NATIONAL AIR INTELLIGENCE CENTER.

PREPARED BY:

TRANSLATION SERVICES
 NATIONAL AIR INTELLIGENCE CENTER
 WPAFB, OHIO

NAIC-ID(RS)T-0412-94

22 February 1995

Date

GRAPHICS DISCLAIMER

All figures, graphics, tables, equations, etc. merged into this translation were extracted from the best quality copy available.

TABLE OF CONTENTS

GRAPHICS DISCLAIMER	i
Table of Contents	ii
High-resolution TeO_2 Acousto-optical Deflector for Millimeter-Wave Spectrometer by Xu Binghuo, Zhao Guozhen, Bian Huian, Chu Haiqun and Jin Jianhui	1

HIGH-RESOLUTION TeO_2 ACOUSTO-OPTICAL DEFLECTOR FOR MILLIMETER-WAVE SPECTROMETER

Xu Binghuo, Zhao Guozhen, Bian Huian, Chu Haiqun, and Jin Jianhui, of Shanghai Institute of Ceramics, Chinese Academy of Sciences

Abstract. This paper introduces high resolution TeO_2 deflector for mm-wave radio spectrometer. We have developed mm-wave acousto-optic radio spectrometer using these devices, it has 17.5 KHz frequency resolution, 13 MHz bandwidth and the system drift is ± 0.03 channel per hour.

Acousto-optical spectrograms are used mainly for radar signal processing and radio spectrum analysis. For this purpose, researchers studied high-frequency band (1 to 2GHz bandwidth) acousto-optical devices and high-resolution acousto-optical devices.

A high-resolution millimeter-wave acousto-optical radio spectro-graph is used to discover and observe fine structures of spectral line clusters of organic molecules and atoms in the universe. This is very valuable for research on star formation and evolution, as well as the origin of life. For this purpose, the authors studied extraordinary Bragg diffraction acousto-optical diffractors based on x-cut LiNbO_3 with TeO_2 as the working medium. In a joint development with the Nanjing Observatory, a millimeter-wave acousto-optical radio spectrograph with resolution of 17.5kHz was developed.

Acousto-optical Interaction in Anisotropic Media

TeO_2 crystals are twinning optical light rotating crystals based on yellow tellurium ore in the 422 crystal system; this is an excellent acousto-optical crystal. Its most primary feature is the propagation of light along the direction of the [110] axis. The acoustic shearing wave oscillating along the direction of the [110] axis has a very low speed of sound (0.616km/s [1]). The low speed of sound brings many advantages. For instance, the characteristic length L_0 is short for acoustic-optical interaction; the scanning angle α of the light beam is large; the number N of distinguishable points is high; and the acousto-optical optimum value M_2 is large. However, for low speed of sound, the transition time τ becomes greater, thus limiting the applications in processing of some fast signals.

The TeO_2 crystal is a birefringent light-rotating crystal. Near the optical axis, the light-rotating property has the main guidance function (optical activity: $87^\circ/\text{mm}$). Upon deviating from the optical axis (for angle of deviation larger than 3°), the birefringence property is the major function. In the crystal, when the incident light interacts with the shearing wave propagating along the [110] direction, extraordinary Bragg diffraction occurs. In other words, the polarization conditions of incident light and diffraction light are different; the incident angle and diffraction angle are different; and the refractive indexes of incident light and diffraction light are different. By comparing the normal Bragg diffraction in homogeneous media, the extraordinary Bragg diffraction not only upgrades the dynamic properties of acousto-optical devices, but also upgrades the bandwidth-efficiency property of the device.

Fig. 1 is a wave vector diagram of acousto-optical interaction in a birefringent crystal. \bar{K}_i and \bar{K}_d represent, respectively, the wave vectors of incident light and of

diffraction light; \vec{K}_d represents the sound wave vector.

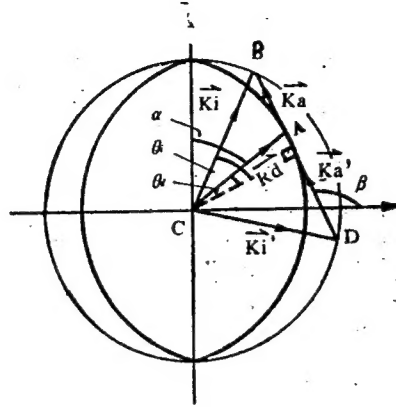


Fig. 1. Acousto-optical interaction wave vectors in a birefringent crystal

Fig. 1. indicates the situation of "tangent-phase match". In other words, the acoustic wave vector is approximately tangent to the ellipsoid of refractive index. Hence, even under the condition that the acoustic wave vector remains unchanged, the phase match of a wide frequency band still can be attained. On the other hand, As shown in $\triangle ABC$ and $\triangle ADC$, there are two tangent-phase matches along the same direction in which the sound wave is propagated. In other words, along the same sound wave direction of propagation, acousto-optical interaction of two different center frequencies are generated. In other words,

$$\vec{K}_i = \vec{K}_d \pm \vec{K}_a \quad (1)$$

$$v_i = v_d \pm f_a \quad (2)$$

In the equations, v_i is the frequency of incident light; v_d is the frequency of the diffraction light; f_a is the sound frequency. " \pm " is determined by the relative position of the directions in which the incident light and sound waves are propagated.

From Fig. 1, by using the cosine law, we can obtain

$$\sin \theta_i = \frac{1}{2 K_i K_d} (\vec{K}_a^2 + \vec{V}_i^2 - \vec{K}_d^2)$$

In the equation,

$$\vec{K}_i = \frac{2\pi n_0}{\lambda_0}, \quad \vec{K}_d = \frac{2\pi nd}{\lambda_0}$$

by substituting into the above equation, we obtain

$$\sin \theta_i = \frac{\lambda_0}{2 n_i \Lambda} \left[1 + \frac{\Lambda^2}{\lambda_0} (n_i^2 - n_d^2) \right] \quad (3)$$

For the same reason,

$$\sin \theta_d = \frac{\lambda_0}{2 n_d \Lambda} \left[1 + \frac{\Lambda^2}{\lambda_0} (n_i^2 - n_d^2) \right] \quad (4)$$

In the equation, the subscripts i and d stand for, respectively, incident light and diffraction light. The subscripts i and d stand for, respectively, the angles of incident light and of diffraction light in the medium related to the array plane of the sound wave.

High-resolution TeO_2 Acousto-optical Deflector

Based on the operating mode, there are two types of acousto-optical deflectors [2]. One type of deflector involves the fact that the supersonic wave propagates along the direction of the [110] axis; the optical wave is incident to the "on-axis type" devices in the direction of the [110] axis. This kind of device has mode degeneracy at the center frequency; concave pits appear in the diffraction bandwidth. Since the center frequency is low, the relative bandwidth is also low. There are other shortcomings such as the requirement of circularly polarized light being incident, due to the light-rotating property. However, for certain special applications, such as the analysis of millimeter-wave acoustic-optical radio spectrogram, there are certain advantages. The main index of the spectrograph is the frequency resolution. Owing to limitations on the number of array elements for photoelectric diode, it is enough for the diffraction bandwidths being approximately 15MHz. Thus, the authors adjust the device's frequency response into signal peak state, or avoid the concave pit zones when using the device. Thus, a flat

frequency response can be satisfactory. On the other hand, the light path in crystals of this type of device is only one-third of that of the "off-axis" type, thus ensuring the image quality of diffraction light. Thus, the widening factor of frequency resolution due to image quality is decreased.

Another type of TeO_2 acousto-optical deflectors is such that the supersonic wave propagates with deviation from the $[110]$ axis; the optical wave is also deviating the optical axis during incidence in the "off-axis" devices. If the deviation angle is properly selected, the mode degeneracy zone can be moved outside of the working bandwidth. Owing to higher center frequency in this type of device, the relative bandwidth is somewhat greater. Besides, since the incident direction of the optical wave deviates from the optical axis, linearly polarized light can be used. These devices are applied mainly in the processing of optical signals. A shortcoming of the "off-axis" device is there is the 51° deviation angle between the wave vector direction and energy flow direction. In order to raise the resolution, the crystal dimensions should be increased. Table 1 lists the performance indices of the TeO_2 deflectors ("on-axis type and off-axis type").

Sound attenuation is disadvantageous to the development of high-resolution TeO_2 acousto-optical devices. The authors discovered that two very disadvantageous phenomena (see Fig. 2) appear when the acoustic shearing wave propagates along the direction of the $[110]$ axis, as shown in Fig. 2). First, with increasing distance along the direction of the $[110]$ axis, the supersonic power peak deviates from the $[110]$ axis; the deviation angle is about $20'$. Secondly, with increasing distance along the $[110]$ direction, the acoustic field diffuses along the $[110]$ direction; moreover, the intensity distribution of the sound field is not uniform.

TABLE 1. Performance Indicators of TeO_2 Acoustic-optical Deflectors

	TD 40 (在轴型) a	TD 70 (离轴型) b
光波波长(μm) c	0.633	0.633
孔径(mm) d	3×65	3×40
激光偏振态 e	右旋圆偏振 l	线偏振 m
中心频率(MHz) f	40	70
衍射效率 g	40%	70%
带宽(MHz) h	25	40
i 时间带宽乘积	2500	2400
频率分辨率(KHz) j	10	17
驱动功率(W) k	1.5	1.5

KEY: a - On-axis type b - Off-axis type c - Optical wavelength d - Aperture e - Laser polarization state f - Center frequency g - Diffraction efficiency h - Bandwidth i - Product of multiplying time by bandwidth j - Frequency resolution k - Driving power l - Polarization of right-handed circle m - Linear polarization

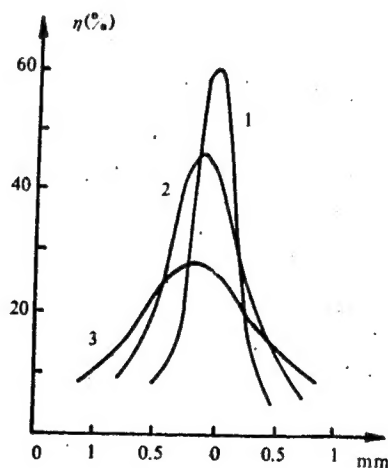


Fig. 2. Variation of sound field power on the horizontal cross-section of TeO_2 deflector
1 - 5mm from transducer 2 - 30mm from transducer
3 - 50mm from transducer

Transducer design of high-resolution TeO_2 acousto-optical deflectors differs from that of conventional deflectors. At the outset, in order to increase bandwidth, the first level tracking system of a four-plate series connection drive was adopted for the transducer. As a result, the frequency response appears as a fluctuation resembling mountain peaks, as shown in Fig. 3. By using the shadow method to observe the distribution of the acoustic field at the device cross section, it was discovered that severe interference phenomena of the acoustic field appears, as shown in Fig. 4a. Looking for its cause, to improve resolution, the dimensions are increased to about 60mm along the [110] direction of the crystal; however, the divergence is greater for the acoustic shearing wave occurring at the four-plate transducer, thus generating interference with superimposition. If the dimension along the [110] direction is less than 20mm, this interference phenomena can be reduced. Later, single-plate or two-plate transducers were employed to improve the interference phenomena of the acoustic field, as shown in Fig. 4b.



Fig. 3. Frequency response at series drive for four-plate transducer

Millimeter-wave Acousto-optical Radio Spectrometer

The acousto-optical radio spectrometer is based mainly on the principle of acousto-optical interaction. The radio signals received from the antenna are fed to the supersonic transducer of the Bragg pool. When the acoustic wave propagates in a medium,

the spectrogram and the intensity properties of the radio signals are preserved. Therefore, an optical simulation diagram is displayed on the focal plane after a Fourier transform of the diffraction light. The simulation graph indicates the power spectrogram of the spectral lines surveyed. Fig. 5 is a block diagram of the system. In the system, the frequency resolution is affected by the following factors, thus broadening the frequency resolution. The first broadening factor is due to the side lobe of the diffraction light. Therefore, the system requires higher image quality on the diffraction light, generally requiring that the side-lobe power level is lower than -18 to -20dB. For deflectors of a certain optical aperture, the effect is different as to resolution due to the light intensity distribution of the laser beam. The resolution is the highest for a homogeneous light beam. However, the side lobe of the image in the diffraction diagram is higher than -12dB. If the truncated distribution gaussian light beam is employed, then it will affect the side lobe so that the image of the diffraction diagram can be reduced in decibels. The authors applied a truncation ratio $\rho=1.5$ ($\rho=D/d_0$, d_0 is the width of the light intensity of the light beam). Now, the side-lobe power level is lower than -20dB. As for the resolution, its broadening factor R is equal to about 1.3. Another reason for the broadening resolution stems from the different special response of light intensity for each array element of the optoelectronic diode array. At this stage, the broadening factor B is related to the number N of array elements included in the half-width of the diffraction light spot. If we assume $N=1.4$, then B is approximately equal to 1.1. In the author's system, D is made to equal 50mm. Now, the theoretical resolution $d_f' = v/D = 12.3\text{kHz}$. Considering the above-mentioned broadening factor, the resolution should be $df = d_f' RB = 17.6\text{kHz}$. At this point, the authors executed gaussian simulation processing in a computer on the system resolution actually measured. The average frequency resolution at the half-power point is 17.5kHz; this matches with the

theoretical analysis. Fig. 6 is an oscillogram of frequency resolution measured by using an optoelectronic diode array, 1.2m focal-length lens, and model 6166 frequency synthesizer.

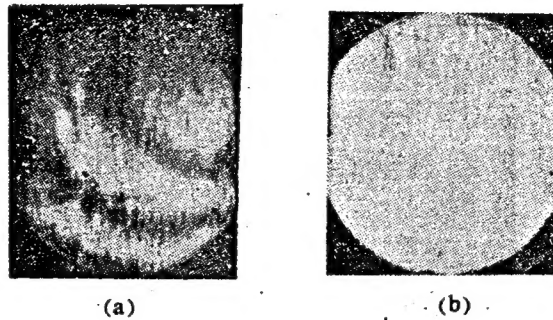


Fig. 4. Distribution of acoustic field on lateral cross-section of TeO_2 acousto-optical deflector observed with shadowgraph method: (a) series drive with four-plate transducer; (b) series drive with two-plate transducer

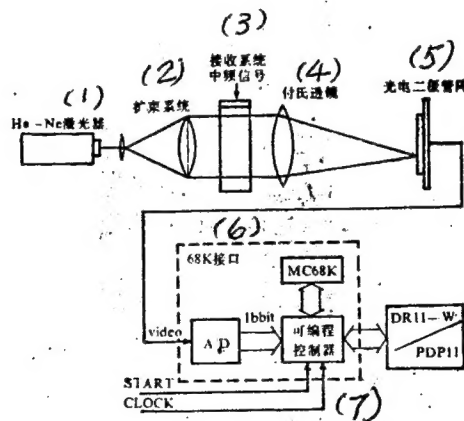


Fig. 5. High-resolution acousto-optical spectrometer
KEY: 1 - Laser 2 - Beam expansion system 3 - Intermediate frequency signal of reception system 4 - Fourier lens 5 - Optoelectronic diode array 6 - Interface 7 - Programmable controller

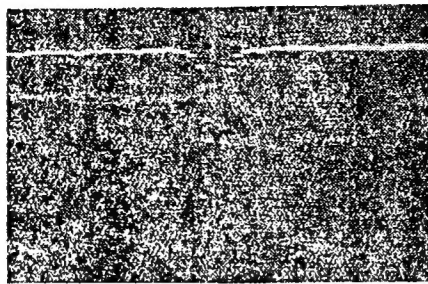


Fig. 6. Frequency resolution oscilloscope

Operations aimed at wave stabilizing in a millimeter-wave acousto-optical radio spectrometer system are very important. Since the opening angle is only 3", corresponding to each array element (15micrometers) of an optoelectronic diode array, thus slight motion of the system will cause channeling. After the authors adopted a double-weight oscillation prevention system, the system drift was lowered to 0.03 of a channel per hour.

The article was received for publication on 13 April 1988.

REFERENCES

- [1] Naoya Uchida, Phys. Rev., B4, 3736 (1971)
- [2] T Yano: Appl. Phys. Lett, 26, 89 (1975)

DISTRIBUTION LIST

DISTRIBUTION DIRECT TO RECIPIENT

<u>ORGANIZATION</u>	<u>MICROFICHE</u>
B085 DIA/RTS-2FI	1
C509 BALLOC509 BALLISTIC RES LAB	1
C510 R&T LABS/AVEADCOM	1
C513 ARRADCOM	1
C535 AVRADCOM/TSARCOM	1
C539 TRASANA	1
Q592 FSTC	4
Q619 MSIC REDSTONE	1
Q008 NTIC	1
Q043 AFMIC-IS	1
E051 HQ USAF/INET	1
E404 AEDC/DOF	1
E408 AFWL	1
E410 AFDTC/IN	1
E429 SD/IND	1
P005 DOE/ISA/DDI	1
P050 CIA/OCR/ADD/SD	2
1051 AFTT/LDE	1
P090 NSA/CDB	1
2206 FSL	1

Microfiche Nbr: FTD95C000077L
NAIC-ID(RS)T-0412-94